Multi-objective Optimization of Volute Springs using an Improved NSGA II

Navid Moshtaghi Yazdani*
Department of Mechanical Engineering,
University of Tehran, Iran
E-mail: navid.moshtaghi@ut.ac.ir
*Corresponding author

Received: 29 March 2020, Revised: 25 July 2020, Accepted: 8 August 2020

Abstract: Due to the variable stiffness through their length, their resistance against buckling, damping characteristics due to the friction between their chains, and their small solid length, volute springs are widely used in applications where other mechanisms cannot be employed to provide variable spring stiffness. Meanwhile, the complexities of equations, governing their dramatic non-linear behavior caused the designers to use experimental equations, as well as some simplifications. Therefore, no research has been reported yet that aims to simultaneously optimize the evaluation criteria of these springs (i.e. their weight and energy conservation capacity) considering their strength, stiffness and natural frequency. In this article providing the governing equations for mechanical behaviors of volute springs, the problem of optimized design for this type of springs are addressed as an optimization problem with its constraints, taking into account the aforementioned goals and considerations. To find a set of Pareto front, an improved version of a multi-objective genetic algorithm is employed, performance of which has been improved, adding a migration operator to a classical NSGA II algorithm. To indicate the proposed method efficiency, a volute spring used in a suspension system of a military motorcar was modeled, and its design was optimized. The results show that the functional performance of the designed volute spring, such as minimizing the spring mass and maximizing the stored energy while maintaining design limitations such as dimensions, strength and critical frequency, has been significantly improved.

Keywords: Military Motorcar, Nsga II Algorithm Improvement, Optimization, Volute Spring

Reference: Navid Moshtaghi Yazdani, "Multi-objective Optimization of Volute Springs Using an Improved NSGA II", Int J of Advanced Design and Manufacturing Technology, Vol. 13/No. 4, 2020, pp. 13–19.
DOI: 10.30495/admt.2020.1896458.1183

Biographical notes: Navid Moshtaghi Yazdani received his MSc in Mechatronic Engineering in the field of control and robotic from University of Tehran. He is currently PhD Candidate at the Department of Electrical Engineering, IAUM University, Mashhad, Iran. More than 16 journal papers, 35 accepted conference papers, and 3 published book are the results of his researches so far. He has been involved in teaching and research activities for more than 10 years in the field of control, robotic and optimization in different universities. His current research interest includes Fault Diagnosis, vibration, optimization and artificial intelligence**.**

1 INTRODUCTION

Volute springs were first widely used in an industrial scale, in suspension systems of lightweight tanks during the world war II [1]. However, their application was changed after the war, and they were widely used in various other applications [2]. This kind of springs has considerable benefits, including low-volume (in the solid-state), ease of manufacturing, damping characteristics due to the friction between the chains, lateral stability, as well as variable spring stiffness (the non-linear nature of the force-displacement graph) [3]. with the ever-increasing demand for building the future generation suspension systems that can use volute springs that have less mass and more stored energy, there is an urgent need for developing volute springs that respect the systems' constraints. However, less mass and stored energy are more than the minimum requirements of each filter for suspension and control purposes, and it is desirable to design a spring that meets the desired performance characteristics of the system.

In recent years, a lot of researches addressed the design, as well as the improvement of volute springs' design methods [4-6]. As well, some studies considered the residual stresses and fatigue strength in these springs [7]. Furthermore, some practitioners considered novel applications of these springs, including the transmission of the command system mechanical signals to the Electronic Control Unit (ECU) in cars [8-9].

In [10], the performance of three nonlinear compliant orthoplanar springs, namely, bi-leg, quad-leg and pent-leg designs are compared to study the vibration mode interaction effect for widening the operational bandwidth of piezoelectric vibration energy harvester. All the designs have three or more vibration modes below 150 Hz with the addition of multiple masses.

On the other hand, some studies have been done to design springs having a similar function to volute springs, lacking some of their drawbacks [11-12]. Despite the importance of optimal volute spring design, spring design with increasing stiffness or spring design with lesser mass are examined separately in a review of the subject literature. This gap between these issues has motivated multi-objective optimization with performance assurance.

In this paper, the specifications of a volute spring used in a military motorcar have been considered as a case study [1]. The range of the spring design parameters is also considered according to a range of parameters for the same spring so that the comparison between the optimized spring parameters and the original spring could be significant. The purpose of optimization is to find a spring that meets the primary design requirements and meanwhile, characterizing a lower mass and a more stored energy compared to the original spring. Reducing the mass and increasing the amount of stored energy in the spring (which is usually associated with an increase in the stiffness), the spring critical frequency also increases. In this article, by adding the migration operator to the NSGA (II) algorithm, the set of non-defeating Parto responses will be improved.

2 VOLUTE SPRING MODELING

A number of equations and figures provided in this section, were borrowed from reference [3] which are mentioned here by citation. Given the spring geometry in "Fig. 1", the spring coil radius follows:

$$r = r_0\left(1-\frac{\beta\theta}{2\pi n}\right) \tag{1}$$

Where, θ is the coil angle, which is measured relative to the external radius. n is the number of the spring active chains. B is obtained as follows:

$$\beta = \frac{r_o - r_i}{r_0} \tag{2}$$

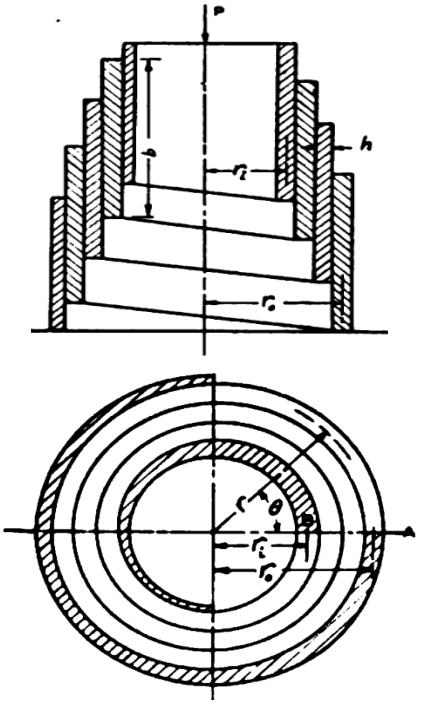

Fig. 1 Lateral cross-section and transverse cross-section of a volute spring.

Where, ro and ri are the external and internal radiuses, respectively "Fig. 1". To calculate the stress and the elongation along a volute spring in practical application, we assume each of its elements as a usual spring having a rectangular cross-section and a radius of the same

element. Thereby, in this method, the friction between chains are ignored. Exceeding the load from a certain value, called the initial bottoming load, the external chains are engaged with the surface which the spring sits on and causes the spring to have a more stiffness. So, the volute spring non-linear characteristic graph tends to return to the bottom chains' bottoming phenomena.

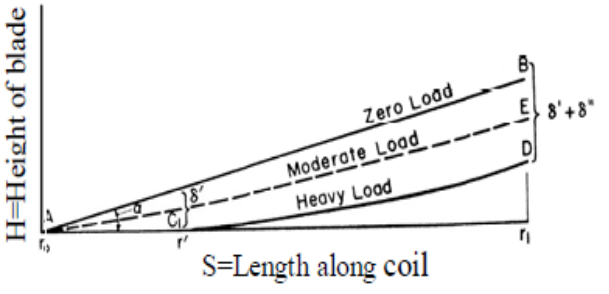

Fig. 2 Height of the spring blade vs. length along coil, in 3 modes: zero loading, a load lower than the initial bottoming load, and a load exceeding initial bottoming load [3].

An approximation for the elongation in each spring active chain having a rectangular cross-section, where the longer edge is parallel to the spring axis, and the cross-section length to width ratio is more than 2.7, is as follows [3]:

$$\delta_t = \frac{6\pi \mathrm{Pr}^3}{Gbh^3\left(1-0.63h/b\right)} \tag{3}$$

Where:
P = the exerted force to the spring,
h = the sheet thickness,
b = the sheet width,
G = the metal stiffness moduli,
R = the spring coil radius

So, for an element of a volute spring having a small angle dθ, the differential change in the spring elongation is obtained as follows:

$$d\delta = \delta_t \frac{d\theta}{2\pi} = \frac{3\pi \mathrm{Pr}^3 d\theta}{Gbh^3\left(1-0.63h/b\right)} \tag{4}$$

Where, r is the spring radius, which is a function of angle θ. According to "Fig. 2", during the bottoming phenomena which is initiated from the spring external radius, the slope dδ/ds should be equal to the coil angle α. As well, since the coil angle is small in volute springs, we have:

$$\left.\frac{d\delta}{ds}\right|_{r=r_0} = \tan\alpha \approx \alpha \tag{5}$$

Assuming r = ro in "Eq. (6)", the initial bottoming load, P_1 is obtained as follows:

$$P_1 = \frac{Gbha\left(1-0.63h/b\right)}{3r_o^2} \tag{6}$$

The spring elongation due to the loading is investigated in two various conditions: first, in a condition where the load is lower than the bottoming load. The second condition is where the load is higher than the bottoming load.

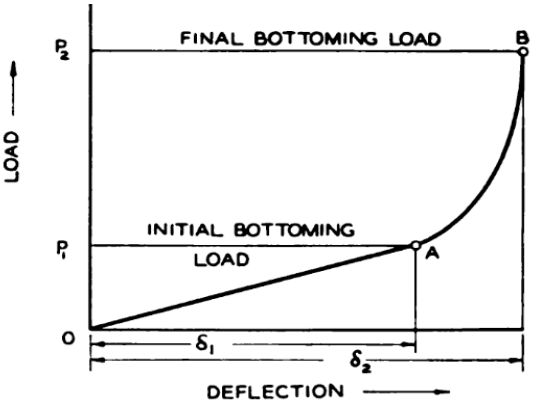

Fig. 3 Spring characteristic graph. The graph shows the spring elongation vs. load, qualitatively.

In case, where P is lower than the bottoming load, we have:

$$d\delta = \frac{3\mathrm{P}r_o^3\left(1-\frac{\beta\theta}{2\pi n}\right)d\theta}{Gbh^3\left(1-0.63h/b\right)} \tag{7}$$

Integrating "Eq. (7)", between 0 and 2πn, yields:

$$\delta = \frac{P}{P_1}\left(2\pi n r_o \alpha K_1\right), \qquad K_1 = 1-1.5\beta+\beta^2-0.25\beta^3 \tag{8}$$

Where, P_1 is the initial bottoming load. Thereby, the spring elongation at the initial bottoming is obtained as:

$$\delta_1 = 2\pi n r_o \alpha K_1 \tag{9}$$

If the spring force is higher than the initial bottoming load, can one consider the resulting elongation in the spring in two parts: the compression δ' that is related to those chains, subjected to bottoming, i.e. AC section in "Fig. 2".

The other part is δ" that is related to the spring free part, subjected to bottoming, that is CD section in "Fig. 2". Assuming that the spring chains are subjected to bottoming with an angle of θ' and a radius of r', and given r=r', we have:

$$c' = 2\sqrt{\frac{Gbha\left(1-0.63h/b\right)}{3P}} \tag{10}$$

Where, c'=2r'/h is the spring index for r=r'. Then, θ' is obtained as follows:

$$\theta' = \frac{2\pi n}{\beta}\left(1-\frac{c'}{c_o}\right) \tag{11}$$

Where, co is the spring index for r=ro. Integrating as follows, can one find δ':

$$\delta' = \int_0^{\theta'} \alpha r d\theta = \alpha r_o \theta'\left(1-\frac{\beta\theta'}{4\pi n}\right) = \frac{\pi\alpha r_o n}{\beta}\left(1-\frac{P_1}{P}\right) \tag{12}$$

To obtain δ", similar equations can be applied. Integrating "Eq. (8)" between θ=θ' and θ=2πn, we have:

$$\delta'' = \int_{\theta'}^{2\pi n} \frac{3pr_o^3(1-\frac{\beta\theta}{2\pi n})^3}{Gbh^3(1-0.63h/b)} d\theta \tag{13}$$

Therefore, the total spring elongation is obtained as follows:

$$\delta = \delta' + \delta'' = 2\pi\alpha r_0 n\left(\frac{P}{P_1}K_1 - \frac{K_2}{\beta}\right)$$
$$K_2 = \frac{1}{2}\left(\frac{P_1}{2P} + \frac{P}{2P_1} - 1\right) \tag{14}$$

The force P_2 under which all spring chains are subjected to bottoming and the spring reaches its solid length, is calculated as follows:

$$\frac{c'}{c_0} = \frac{r'}{r_0} = \sqrt{\frac{P_1}{P}} \tag{15}$$

When r=ro, all chains are subjected to bottoming. So, one can find the final bottoming load as follows:

$$P_2 = \frac{P_1}{(1-\beta)^2} = P_1\left(\frac{r_o}{r_i}\right)^2 \tag{16}$$

The final elongation δ2 due to the force P_2 can be calculated, assuming θ'=2πn and then integrating:

$$\delta_2 = \int \alpha r_o\left(1-\frac{\beta\theta}{2\pi n}\right)d\theta = 2\pi n\alpha r_o\left(1-\frac{\beta}{2}\right) \tag{17}$$

The resulted value is in fact the difference between the spring free length and its solid length. Rewriting this equation in terms of α, we have:

$$\alpha = \frac{\delta_2}{2\pi n r_o\left(1-\frac{\beta}{2}\right)} = \frac{H-b}{2\pi n r_o\left(1-\frac{\beta}{2}\right)} \tag{18}$$

Stored energy in the spring: the energy stored in the spring is equal to the area under the force-displacement graph. In the region where the spring elastic behavior is linear, we simply have:

$$E_{0-1} = 0.5P_1\delta_1 = \pi G\,\frac{K_1 nbh^3\alpha^2\left(1-\frac{0.63h}{b}\right)}{3r_o} \tag{19}$$

Where, $E_{0\text{-}1}$ is the energy stored in the spring from initial loading until bottoming initiation (linear region on the graph). In the non-linear region, that is from bottoming initiation until the spring reaches its solid length, the equation governing the spring force and its elongation is as follows:

$$\delta = 2\pi\alpha r_o n\left(K_1\frac{P}{P_1} - \frac{P_1}{4\beta P} - \frac{P}{4\beta P_1} + \frac{1}{2\beta}\right) \tag{20}$$

Given "Eq. (20)" and calculation of the following integral, $E_{1\text{-}2}$, that is the energy stored in the spring from bottoming initiation until it reaches its solid length is obtained.

$$d\delta = 2\pi n\alpha r_o n\left[\left(\frac{K_1}{P_1} - \frac{1}{4\beta P_1}\right)dP + \frac{P_1}{4\beta P^2}dP\right]$$
$$\rightarrow E_{1-2} = \int_{\delta_1}^{\delta_2} P d\delta = 2\pi n\alpha r_o n\left[\left(\frac{K_1}{P_1} - \frac{1}{4\beta P_1}\right)\frac{P^2}{2} + \frac{P_1}{4\beta}\ln(P)\right]_{P=P_1}^{P=P_2} \tag{21}$$

Summing up E0-1 and E1-2, the energy stored in the spring is calculated. The other objective function is the spring's mass, which can be simply obtained according to the spring's geometry, as follows:

$$m = \rho hb \frac{H - b}{\tan(\alpha)} \cos(\alpha) \quad (22)$$

Stress: to calculate stresses in a volute spring, the same equations as the coil springs having a rectangular cross-section are used.

When the spring force is lower than the initial bottoming load, the maximum stress occurs in $r=r_o$. In such a case, an approximation is as follows [3]:

$$\tau = \frac{3P(c_o + 1)}{2hb(1 - \frac{0.63h}{b})} \quad : P<P_1 \quad (23)$$

As well, when the spring force exceeds the initial bottoming load, the maximum shear stress occurs in r=r'. Therefore, replacing co by c' and using the previous equation, we have:

$$\tau = \frac{3P(c' + 1)}{2hb(1 - \frac{0.63h}{b})} \quad ; c'=2r'/h \ : P>P_1 \quad (24)$$

According to "Eq. (16)":

$$\tau = \frac{3P(c_O \sqrt{P / P_1} + 1)}{2hb(1 - \frac{0.63h}{b})} \quad : P>P_1 \quad (25)$$

If all spring chains are subjected to the bottoming, that is the spring reaches its solid length, then P=P2. Thus, the maximum shear stress is obtained at the spring final bottoming:

$$\tau = \frac{3P_2(c_i + 1)}{2hb(1 - \frac{0.63h}{b})} \quad (26)$$

Where, c_i is the spring index at $r=r_i$. Putting P_2 and P_1 in "Eq. (26)", we have:

$$\tau_2 = \frac{3G\alpha(c_i + 1)}{{c_i}^2} \quad (27)$$

3 OPTIMIZATION METHOD

Due to the broad dimensions of search space, multi-modal nature of the objective function, as well as multiple local optimums in the search space, the classical optimization algorithms are seriously prone to be entrapped in local optimums. Therefore, it is usually preferred to employ population optimization rather than classical methods, because they can find optimal region(s) for functions with a considerable speed and can approach absolute optimum(s), even in the case of non-convex functions. These algorithms use a set of monitoring points in their process and do not need any objective function's derivative [13-14]. In this study, adding an immigration operator to other common operators in genetic algorithm (i.e. selection, crossing-over, and mutation), the soft mean of the utopia compromise point was improved up to 90% after 100 execution efforts of the optimization code, based on the main and improved algorithms of NSGA II.

Table 1 A subset of Pareto front set as a result of optimization. The basic spring specifications are highlighted blue

b (mm)	h	r_i (mm)	n	α (rad)	E (J)	M (kg)	τ (Mpa)
50	4	50	5	0.025	14.889	2.96	175
62.5	4	49	4	0.026	15.436	2.81	176.3
59.5	4	51	4	0.027	15.410	2.77	176.3
58	4	52	4	0.027	15.344	2.75	176.4
56.5	4	53	4	0.028	15.233	2.72	176.2
62.5	4	53	3.5	0.028	15.088	2.59	176.5
55.5	4	58	3.5	0.031	14.751	2.49	176.1
62.5	4	58	3	0.031	14.481	2.37	175.8
61.5	4	59	3	0.031	14.326	2.37	174.6

4 RESULTS

A set of springs to be replaced by the basic spring, based on the conditions mentioned in the problem description, is summarized in "Table 1". As can be seen, the value for the mass objective function, as well as the maximum shear stress are located in a range similar to the range of corresponding one in basic springs. In "Table 1", springs 1-5 have lower mass value and a more amount of stored energy compared to the basic spring. The mass and the stored energy for other springs in the Pareto front are more different from their corresponding values in the basic spring. However, they offer the decision-maker a more extensive range to select from, in his/her design effort.

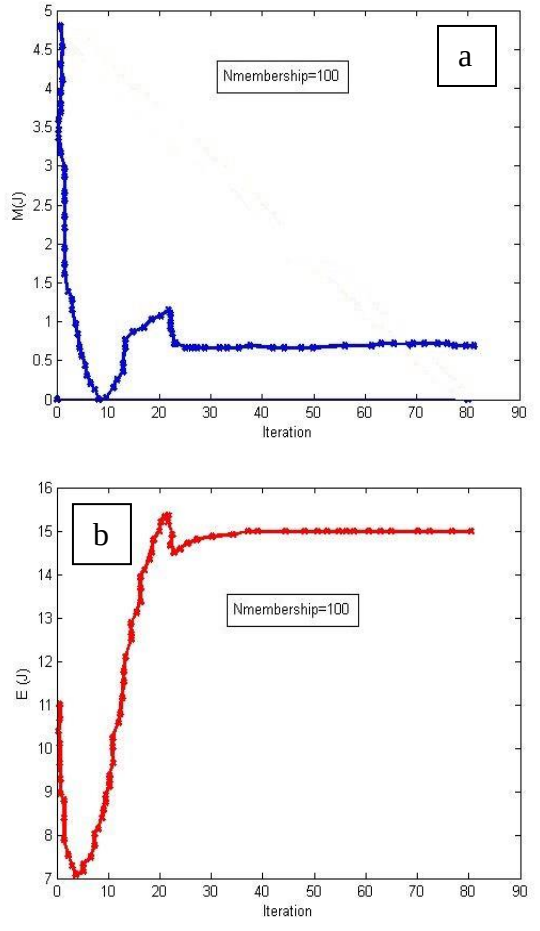

Fig. 4 (a) The average amount of the stored energy for a single generation's members as the generations advance (number of members in a single generation = 100). As can be seen, this objective function increases as the generations advance, and (b): the average value of mass for a single generation's members as the generations advance (number of members in a single generation = 100). As can be seen, this objective function decreases as the generations advance.

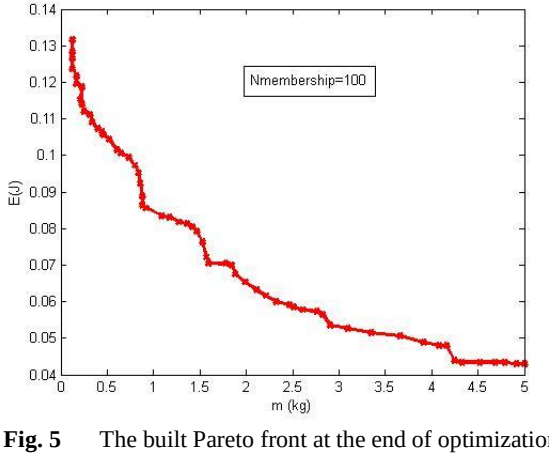

Fig. 5 The built Pareto front at the end of optimization (the number of members in a single generation = 100). Since the energy quantity is maximized, the inverse for this quantity is shown on the vertical axis of this graph.

"Table 1" lists three samples for these members. Figures 4-6, indicate the average stored energy in springs (all members of a single generation), the average of the mass objective function, and the final Pareto front, respectively. As can be seen in these graphs, during the optimization process through various generations, the average value of mass decreases and the average amount of stored energy increases.

5 CONCLUSION

Providing analytical equations for designing volute springs in this paper, the design of these springs was addressed as an optimization problem with its constraints, in which the spring's mass and the maximum stored energy are considered as objectives to be optimized, and other design requirements, that is its strength and the critical frequency were taken into account as constraints. To find a set of Pareto optimal solutions, an improved NSGA II algorithm was employed, performance of which was improved adding the genetic immigration operator. This new operator can effectively prevent the algorithm to entrap in local optimums. To demonstrate the efficiency of the proposed approach, the design of a volute spring employed in a military motorcar was investigated. Furthermore, generating a set of non-dominated solutions rather than a single solution, the proposed approach offers the designer to choose a suitable design based on other criteria, such as manufacturing cost.

REFERENCES

[1] Schreier, J. R., Konrad, F., Standard Guide to U.S. World War II Tanks & Artillery, 1st ed, Krause Publications,USA,1994, pp. 154–196, ISBN: 0873412974.

[2] Agachev, A. R., Daishev, R. A., Levin, S. F., et al., First-Level Dulkyn Gravitational Wave Detector, Vol. 52, No. 10, 2009, pp. 613–620, https://doi.org/10.1007/s11018-009-9316-1.

[3] Wahl, A. M., Mechanical Springs, 2nd ed, McGraw Hill, New York, 1963.

[4] Kazunori, K., Spring Standards by The Japan Spring Manufacturing Association and The Points in Designing, the Fourth. Hot Formed Volute Springs, Machine Design, Vol. 42, No. 6, 2002, pp. 97-101.

[5] Sterne, B., Characteristics of the VOLUTE SPRING, SAE Technical Paper 420100, 1942, https://doi.org/10.4271/420100.

[6] Sileikis, W., Volute Spring Design, Bulletin of Military Technical Academy, 2015, pp. 97-104.

[7] Kirpichev, V. A., Akiljuk V. S., Surhuanova, Yu. N., and Karaneva, O. V., Residual Stresses and Fatigue Resistance of Cylindrical Volute Springs, VestnikSamarskogo Gosudarstvennogo Seriya Fisiko-MatematicheskieNauki, Vol. 2, No. 17, 2008, pp. 254-257, https://doi.org/10.14498/vsgtu618.

[8] Reck, C., Mueller, M., and Seipel, V., US Patent Application for a "Vehicle", Docket No.20,070,173,078. Published on 26 July, 2007.

[9] Peng, Q. I., Chen, Q., Hongbin, L., Jian, S. D., et al, A Novel Continuum Manipulator Design Using Serially Connected Double-Layer Planar Springs, IEEE/ASME Transactions on Mechatronics, Vol. 21, No. 3, pp. 1281 – 1292.

[10] Sharvari Dhote, Haitao, L., Zhengbao Y., Multi-Frequency Responses of Compliant Orthoplanar Spring Designs for Widening the Bandwidth of Piezoelectric Energy Harvesters, International Journal of Mechanical Sciences, Vol. 157–158, 2019, pp 684-691, ISSN 0020-7403, https://doi.org/10.1016/j.ijmecsci.2019.04.029.

[11] John, J. P., Larry L. H., and Spencer, P. M., Ortho-Planar Linear-Motion Springs, Mechanism and Machine Theory, Vol. 36, No. 11-12, 2001, pp. 1281-1299,https://doi.org/10.1016/S0094 114X(01) 00051-9.

[12] Ruizhou, W., Xianmin, Z., Optimal Design of a Planar Parallel 3-DOF Nanopositioner with Multi-Objective, Mechanism and Machine Theory, Vol. 112, 2017, pp. 61-83, ISSN 0094-114X, https://doi.org/10.1016/j.mechmachtheory.2017.02.005.

[13] Arora, J. S., Introduction to Optimum Design,5th ed, Elsevier Academic Press, San Diego, California, 2004, ISBN: 9780120641550

Holland, J. H., Adaption in Natural and Artificial Systems,1st ed, MIT Press, Cambridge, MA, 1992.